Molecular Orientation Distribution in Injection-Molded Polycarbonate Discs

MIKIO TAKESHIMA and NOBUHIRO FUNAKOSHI, *NTT Ibaraki Electrical Communication Laboratory, Nippon Telegraph and Telephone Corporation, Tokai, Ibaraki, 319-11, Japan*

Synopsis

The molecular orientation distribution of injection-molded polycarbonate discs is studied using birefringence and heat-shrinkage measurements and laser-Raman spectroscopy. Birefringence and heat shrinkage, which result from the molecular orientation, increase as the distance from the inflow gate decreases and as cylinder temperature decreases. Molecular orientation is reduced following annealing. Laser-Raman spectroscopy is used to measure the molecular orientation distribution along the disc cross-section perpendicular to the radial direction of disc. The relative intensity ratio for the 635 cm^{-1} and 703 cm^{-1} peaks in the Raman spectra correlate well with the degree of molecular orientation. The disk cross-section is found to consist of three different molecular orientation zones; a skin zone which is in contact with the mold, a core zone located at the center, and a shear zone between the skin and the core zones. Molecules in the skin zone are nonoriented while the orientation of molecules in the core zone is considerably relaxed. The shear zone consists of highly oriented molecules. The formation process of the molecular orientation distribution is discussed in relation to birefringence and heat shrinkage.

INTRODUCTION

Polycarbonate is expected to be the most suitable disc substrate material for optical discs[1,2] because it possesses characteristics superior to other plastic materials in terms of dimensional stability,[2] thermal reliability,[2] strength, and low water absorption. Polycarbonate substrate is usually formed by injection molding. However, in many cases, injection-molded polycarbonate substrate exhibits large birefringence,[1] which is caused by the molecular orientation generated during the manufacturing process. This is because polycarbonate possesses a larger photoelastic constant than other plastic materials due to its polarizable anisotropy. To reduce the birefringence, it is necessary to improve the molding conditions.

It is well known that in injection molding the molecular orientation distributes in the thickness direction during the molding process according to the flowability and cooling conditions of molten resin in the mold cavity.[3] The degree of molecular orientation can also be expressed by the birefringence and the heat-shrinkage parameter.[1,4] Therefore, it is assumed that birefringence and heat shrinkage vary according to the degree and the distribution of molecular orientation existing in the thickness direction. To clarify the flowability and the cooling properties of molten resin and the formation process of molecular orientation, it is necessary to quantify the degree and distribution of molecular orientation in the thickness direction. However, it is difficult to detect the molecular orientation distribution di-

Journal of Applied Polymer Science, Vol. 32, 3457–3468 (1986)
 CCC 0021-8995/86/023457-12$04.00

rectly from either the birefringence or the heat shrinkage. Generally, polarized microscopic observation of the cross-section of injection moldings has been utilized to estimate the degree of molecular orientation.[5] This method is, however, unsuitable for accurately determining the distribution of molecular orientation because it provides only qualitative information. This paper proposes that polarized laser-Raman spectroscopy by applied to analyze the degree and distribution of molecular orientation existing in the thickness direction. This technique can provide information about the molecular levels as measured in the vibrational and rotational states of the molecular segment. A number of recent studies have therefore used Raman scattering to characterize the density, degree of crystallinity, and molecular orientation in drawn polymers.[6-8] However, to date, this technique has not been applied to injection moldings using amorphous polymer, such as polycarbonate.

This paper examines the degree and distribution of molecular orientation in the thickness direction of injection-molded polycarbonate discs. Birefringence, heat shrinkage, and laser-Raman spectroscopy measurements were used in this investigation. Furthermore, the flowability and cooling properties of molten resin and the formation process of molecular orientation in the mold cavity are discussed.

EXPERIMENTAL

Injection Molding of Polycarbonate Discs

The material used in this study was *bis*-phenol-A polycarbonate and is shown in Figure 1 (average molecular weight: 25,400; Iupilon polycarbonate, Mitsubishi Gas Chemical Co.). An effort was made to prevent contamination and moisture absorption which might occur before or during the injection molding process. The 1.5-mm thick, 300-mm outer diameter discs shown in Figure 2 were molded with a screw-type injection molding machine (Toshiba Machinery Co., 200-ton locking pressure). The inflow gate for the molten resin is located at the center of the circular cavity. The injection molding conditions are shown in Table I. A typical pressure–time representation of the molding cycle in this study is given in Figure 3.

Birefringence Measurement

The phase change, $\Delta\delta$, was measured at room temperature by ellipsometry using a He-Ne laser at a wave length of 633 nm. Measurements were made along the disc diameter in the direction of molten resin flow. The sample face was irradiated perpendicularly with polarized light. The phase change, $\Delta\delta$, was estimated using the following equation to be the difference between the two main refractive indices, Δn:

$$\Delta n = (\lambda/2\pi d)\,\Delta\delta \tag{1}$$

where λ is the wave length of the incident light and d is the sample thickness.

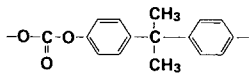

Fig. 1. *Bis*-phenol-A polycarbonate molecular structure.

Heat-Shrinkage Measurement

Specimens were cut from the discs as shown in Figure 2 and annealed at 160°C for 7 h in an air atmosphere. The heat shrinkage, H, was estimated by the following equation:

$$H = \frac{L_0 - L_1}{L_0} \times 100 \tag{2}$$

where L_0 and L_1 are sample lengths measured at room temperature before and after annealing, respectively.

Laser-Raman Spectroscopy Measurement

The Raman spectrum was measured at room temperature using the setup shown schematically in Figure 4. The Raman spectrometer was a Japan Spectroscopic Model R-800 equipped with a double monochrometer. The light source was an NEC Model GLG-3202 Argon Ion Laser (λ = 515 nm) powered by an NEC Model GLS 3200 Exciter. Rated laser output power was about 300 mW. The diameter of the focused laser beam was about 10 μm. All spectra were recorded after several time integrations in order to eliminate the effect of laser noise.

RESULTS AND DISCUSSION

Birefringence and Heat Shrinkage

It has been postulated that birefringence is due to the orientation of molecular groups having polarizable anisotropy.[9] The polarizable anisotropy of the polycarbonate molecule is predominantly associated with its phenyl backbone chain, as shown in Figure 1. Figure 5 shows the birefringence dependence on the distance from the inflow gate (gate distance, L). The birefringence value increases gradually with decreasing gate distance, indicating that the molecular orientation, which is principally re-

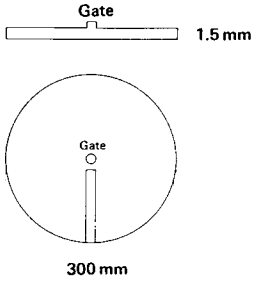

Fig. 2. Dimensions of the injection moldings and sample location.

TABLE I
Injection Molding Conditions

Molding conditions	Experimental no. 1	2	3
Cylinder temperature, T_c (°C)	275.0	305.0	341.0
Mold temperature, T_m (°C)	60	60	60
Holding pressure, P_h (kg/cm^2)	20	20	20
Injection rate, R_i (cm^3/s)	350	350	350
Holding time, H_t (s)	1.0	1.0	1.0

sponsible for birefringence, is greater near the gate. Also, it can be seen that the birefringence value decreases markedly with increasing cylinder temperature (T_c). The oriented molecules are relaxed to some extent in the holding period (C in Figure 3) by the segmental motion of the molecules because the resin temperature still remains high enough to prevent the molecular orientation from being frozen (annealing effect). This phenomena occurs in the temperature range above the glass transition temperature (T_g), in polymers. The extent of relaxation can be controlled mainly by the initial temperature of the molten resin (i.e., the cylinder temperature). Therefore, it is concluded that the higher the cylinder temperature, the more the molecular orientation caused by the holding pressure is relaxed to some extent during the keeping period at high temperature and the more the birefringence value decreases, as shown in Figure 5.

As the result of heat treatment in the temperature range above T_g, molecular chains in the orientation state return to the random coil state as a result of the segmental motion of molecules and the molded articles then shrink. Figure 6 shows the heat-shrinkage dependence on cylinder temperature. The heat shrinkage decreases markedly with increasing cylinder temperature. This result shows that the molecular orientation caused by the holding pressure is relaxed with increasing cylinder temperature as a result of annealing. This is consistent with the birefringence results shown in Figure 5.

Relationship Between Raman Spectra and Birefringence

Figure 7 shows the typical Raman spectrum for injection-molded *bis*-phenol-A polycarbonate in the 500 cm^{-1} to 1800 cm^{-1} range. The observed Raman spectral peaks are usually seen in *bis*-phenol-A polycarbonate. Gen-

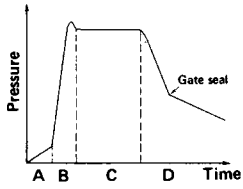

Fig. 3. Variation of pressure with time in injection molding. A: filling, B: packing, C: holding, D: cooling

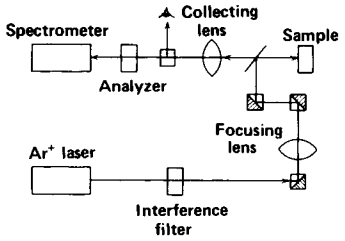

Fig. 4. Arrangement of equipment for laser-Raman spectroscopy.

erally, some of the Raman spectral peaks of polycarbonate can be assigned to benzene ring vibration because the C=C bond has a high symmetry and the vibration mode can be clearly seen in Raman scattering.

It has been postulated that the Raman spectra indicating the rotation and vibration state of molecules are related to the molecular orientation, which is responsible for the birefringence.[12] As shown in Figure 8, θ is defined as the angle between the polarization direction of the incident laser beam and the axis of molecular orientation (the flow direction of molten resin). The laser beam irradiated the sample surface perpendicularly. Figure 9 shows the relationship between Raman peak intensities for $\theta = 0$ and $\theta = 45$. It is clear that there is a θ-dependent group (the Raman peak intensities at 703–1235 cm^{-1}) and an θ-independent group (the Raman peak intensities at 635 and 1600 cm^{-1}). This means that the Raman peak intensities in the θ-dependent group are a good index for estimating the molecular orientation. Here, the relative intensity ratio between the θ-dependent group and the θ-independent group is very effective to be minimally affected by changes in laser beam intensity, sample surface condition, and optical and environmental conditions. The 635 cm^{-1} and 703 cm^{-1} peaks which are adjacent peaks in Figure 7 were examined in this study. Figure 10 shows θ dependences on the relative intensity ratio, $I(703\ cm^{-1})/(635\ cm^{-1})$ of two samples with large birefringence ($\Delta n = 5.3 \times 10^{-5}$) and small birefringence (Δn = zero). It is clear that the relative intensity ratio of the sample showing large birefringence changes sinusoidally with the change of θ. On the other hand, the relative intensity ratio of the sample showing small birefringence is almost independent of θ. Figure 11 shows a good correlation between birefringence and ΔI under $\Delta n = 5.7 \times 10^{-5}$. Accordingly it is possible to observe the degree of birefringence, namely, the degree of molecular orientation, by measuring the relative intensity ratios at $\theta = 45$ or $\theta = 135$.

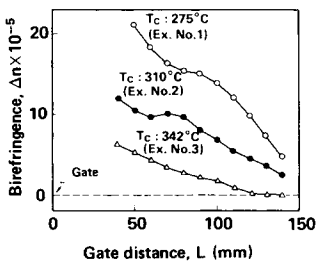

Fig. 5. Birefringence distribution along disc diameter.

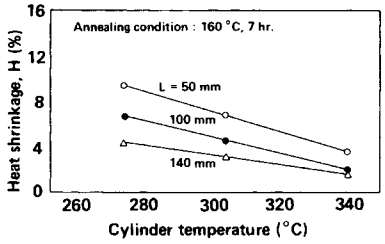

Fig. 6. Dependence of heat shrinkage on cylinder temperature at various gate distances.

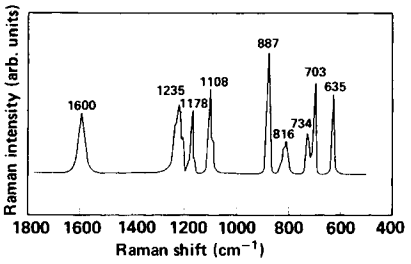

Fig. 7. Raman spectrum of injection-molded polycarbonate.

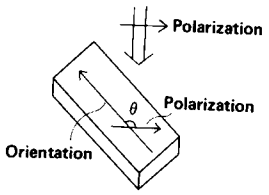

Fig. 8. Geometry of the incident beam.

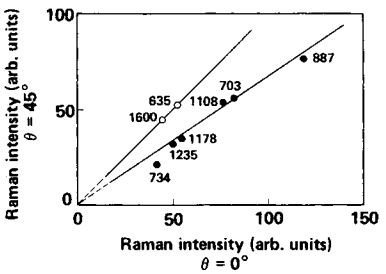

Fig. 9. Dependence of Raman peak intensities on θ. Raman peak intensities at 635 and 1600 cm^{-1} are independent of θ. Other Raman peak intensities are dependent on θ.

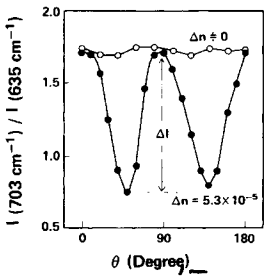

Fig. 10. Dependence of Raman relative intensity ratio on θ. ○, $\Delta n = 0$; ●, $\Delta n = 5.3 \times 10^{-5}$. ΔI is the amplitude of relative intensity ratio change.

Molecular Orientation Distribution Along Disc Cross-section

Changes in the relative intensity ratio were measured along a cross-section perpendicular to the radial direction of the disc. Raman spectra for the 703 cm^{-1} and 635 cm^{-1} peaks from several positions on a disc cross-section are shown in Figure 12. It is evident that the 703 cm^{-1} peak intensity varies along the disc cross-section while the 635 cm^{-1} peak intensity shows almost no change. Figure 13 shows the distribution of the relative intensity ratio, $I(635\ cm^{-1})/I(703\ cm^{-1})$ on the cross-section at several gate distances for example No. 3. The relative intensity ratio at $L = 140$ mm (Δn = zero) shows a nearly constant value. However, the relative intensity ratio at $L = 100$ mm ($\Delta n = 1.8 \times 10^{-5}$) and $L = 40$ mm ($\Delta n = 5.3 \times 10^{-5}$) changes along the disc cross-section. Figure 14 shows a graphic interpretation of the relative intensity ratio distribution for the results shown in Figure 13. There are three zones in this relative intensity ratio distribution: a skin zone, a shear zone, and a core zone. The skin zone consists of nonoriented molecules. In the core zone, the molecular orientation is considerably relaxed. It is interesting to note, however, that the core zone is not always located at the center of the cavity space as shown in Figure 13. This is thought to be caused by nonuniformity in the flow velocity and temperature of the molten resin in the cavity. The shear zone between the skin zone and the core zone consists of highly oriented molecules. The degree of molecular orientation depends on the molding conditions as shown in Table I. Accordingly, the flowability and cooling characteristics of molten resin in the mold cavity during the injection molding process can be estimated by measuring this relative intensity ratio distribution.

In measuring birefringence, the laser beam strikes the sample perpendicular to the sample surface and passes through the sample. Therefore, the measured birefringence can be considered to be the total sum of the locally existing birefringences along the thickness direction. On the other hand, Raman shifts are measured at each depth in the thickness direction, so the total sum of the deviations from the Raman shift in the nobirefringence sample, S, as shown in Figure 14 must be fitted to the birefringence. Figure 15 shows a good correlation between birefringence and S. This result means that both Raman scattering and birefringence result from the same cause, that is, from the molecular orientation.

Heat shrinkage, which is one parameter of molecular orientation, is the average value of the molecular orientation at each point in the cross-sectional distribution. Figure 16 shows very good agreement between heat shrinkage and S. In Figure 15, S does not reach zero when the birefringence

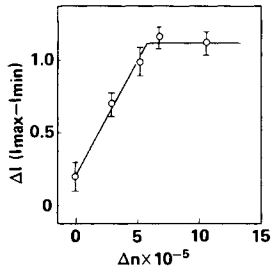

Fig. 11. Dependence of ΔI on birefringence.

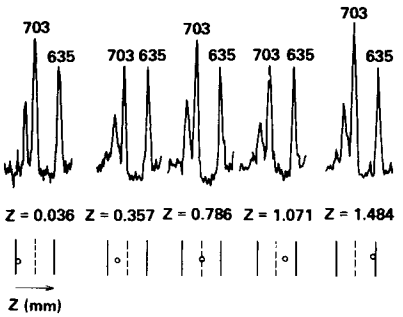

Fig. 12. Raman spectra at different locations along an injection-molded polycarbonate disc cross-section. The position of the laser beam irradiation on the cross-section is shown schematically below each spectrum. Measuring point is the position at $L = 50$ mm of sample no. 3.

value is extrapolated to zero. The same relationship is also seen between birefringence and heat shrinkage, that is, heat shrinkage is about 0.6% when the birefringence is extrapolated to zero.[1] The most reasonable explanation for these phenomena concerning S and the molecular orientation parameter, H, is that the orientation of molecular groups having polarizable anisotropies, from which birefringence arises, are frozen in a more disordered state than that of molecular main chains by cooling of molten resin as pointed out by Koda.[4]

The molecular orientation returns to the random state following heat treatment.[10] The apparent molecular orientation distribution along the disc cross-section [Fig. 17(a)] disappears after heat treatment at 160°C for 7 h [Fig. 17(b)].

Flowability of Molten Resin and the Molecular Orientation Formation Process

The flow behavior of molten resin in the radial and circular direction during the packing period (Fig. 18) can be expressed by the following equation: In the radial direction,

$$\{\pi(L + dL)^2 - \pi L^2\} D = Q\,dt \tag{3}$$

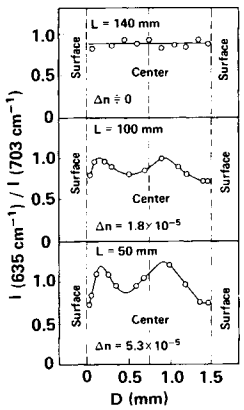

Fig. 13. Change in Raman relative intensity ratio along the disc cross-section by laser-Raman spectroscopy.

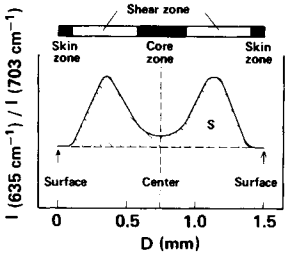

Fig. 14. Cross-sectional frozen orientation profile.

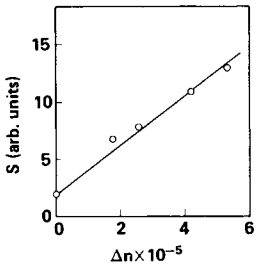

Fig. 15. Relationship between integration value of molecular orientation distribution, S, and birefringence.

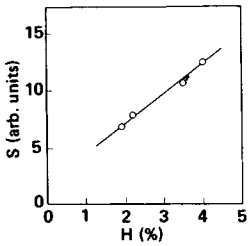

Fig. 16. Relationship between S and heat shrinkage.

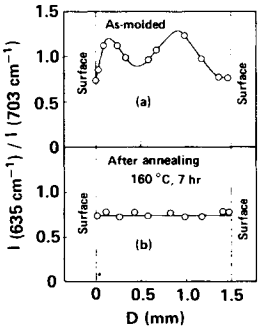

Fig. 17. Disappearance of molecular orientation distribution following heat treatment. (a) As-molded; (b) after heat treatment at 160°C for 7 h.

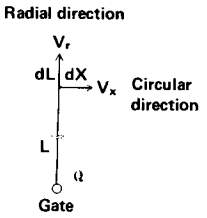

Fig. 18. Flow behavior of molten resin in the mold cavity. Vr = flow velocity in the radial direction. Vx = flow velicity in the circular direction.

where L is the gate distance, Q is the amount of molten resin injected per unit time from the gate, and D is the cavity thickness. dL^2 can be neglected because it is very small. In the circular direction,

$$2\pi(L + dL) - 2\pi L = dX \tag{4}$$

where X is the distance in the circular direction.

From Eq. (3), the flow velocity, Vr, of the molten resin in the radial direction can be expressed as:

$$Vr = \frac{dL}{dt} = \frac{Q}{2\pi LD} \tag{5}$$

where t is the time. Also, from Eq. (4), the flow velocity, Vx, of the molten resin in the circular direction can be expressed as:

$$Vx = \frac{dX}{dt} = 2\pi \frac{dL}{dt} = \frac{Q}{LD} \tag{6}$$

From Eqs. (5) and (6), the flow velocity ratio of molten resin in the circular and radial direction can be derived as:

$$Vx/Vr = 2\pi = 6 \tag{7}$$

Therefore, it is assumed that the greater part of the molecules orient in the circular direction, because the molecular orientation is proportional to the flow velocity of the molten resin, and the degree of orientation is greater near the gate as estimated from Eq. (6). However, molecules oriented in the circular direction relax as a result of the annealing effect in the mold cavity because the resin temperature still remains relatively high. This relaxation phenomenon is also the same in the radial direction. Therefore, the molecular orientation caused by the inflow shear strain during the packing period is not completely frozen.

Molecules oriented during the holding period begin to solidity because the molten resin cools rapidly, and the molecular orientation is frozen. Koda[5] pointed out that the molecular orientation is formed by a backflowing shear strain if the holding time is too short. The results presented here support Koda's thinking. It is assumed that the molecular orientation

caused by the backflowing shear strain during the holding period is responsible for a large part of the molecular orientation in the molded article.

Figure 19 shows a schematic model of the appearance of molecular orientation in the mold cavity during the holding period. The layer in contact with the cold mold wall solidifies rapidly before it suffers shear stress because its cooling rate is very high. Therefore, a very thin nonoriented layer is formed as a skin zone (Fig. 14). The central layer consists of molecules whose orientation is partly relaxed as a result of annealing because the cooling rate for this layer is lowest. The layer between the skin zone and the core zone consists of highly oriented molecules because it suffers high shear stress due to the solidified skin layer, and the cooling rate is relatively high. Figure 20 shows the flow velocity and shear rate distribution profile of molten resin in the mold cavity presented by Wiegand and Vetter.[11] Assuming that the degree of shear stress is equivalent to that of molecular orientation, the results in Figure 13 show a profile similar to that of the shear rate profile in Figure 20(c). Therefore, the relative intensity ratio distribution along the disc cross-section obtained by laser-Raman spectroscopy is thought to express the true molecular orientation distribution.

SUMMARY

The principal findings in this investigation can be summarized as follows:

1. Birefringence and heat shrinkage, which are caused by the molecular orientation, increase as the gate distance decreases. Also, these properties decrease markedly as cylinder temperature increases.

2. Molecular orientation is greater near the gate, and becomes smaller due to the annealing effect in the mold cavity as the cylinder temperature increases.

3. By laser-Raman spectroscopy measurement, the apparent molecular orientation distribution along the disc cross-section perpendicular to the flow direction of molten resin has been obtained using the relative intensity ratio, $I(635\ \text{cm}^{-1})/I(703\ \text{cm}^{-1})$. This shows that there are three molecular orientation zones: a skin zone, a shear zone, and a core zone. Also, the integrated value of the apparent molecular orientation distribution cor-

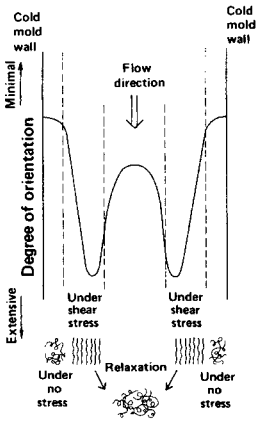

Fig. 19. Schematic representation of molecular orientation in injection moldings.

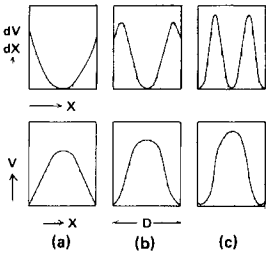

Fig. 20. Velocity profile V and shear rate profile dV/dX: (a) Isothermal flow; (b) surface zones begin to cure; (c) surface zones are already cured.

relates well with birefringence and heat shrinkage. In addition, the apparent molecular orientation distribution disappears following heat treatment at 160°C for 7 h.

4. Molecular orientation is assumed to be formed mainly by a backflow shear strain occurring during the holding period.

Reference

1. M. Takeshima and N. Funakoshi, *Proc. SID*, in preparation.
2. M. Takeshima, T. Okada, and S. Fukunishi, *ECL Rev.*, **32**(2), 253 (1984).
3. M. R. Kantz, H. D. Newman, Jr., and F. H. Stigale, *J. Appl. Polym. Sci.*, **16**, 1249 (1972).
4. H. Koda, *J. Appl. Polym. Sci.*, **12**, 2257 (1968).
5. M. Fujiyama and S. Kimura, *Kobunshi Ronbunshu*, **32**(10), 581 (1975), (in Japanese).
6. S. W. Cornell and J. L. Koenig, *J. Appl. Phys.*, **39**, 4883 (1968).
7. A. J. Melveger, *J. Polym. Sci.*, **10**, (A-2), 317 (1972).
8. J. Purvis and D. I. Bower, *J. Polym. Sci., Polym. Phys. Ed.*, **14**, 1461 (1976).
9. R. D. Andrews and T. J. Hammack, *J. Polym. Sci.*, **C-5**, 101 (1963).
10. M. Takeshima and N. Funakoshi, *Kobunshi Ronbunshu*, **42**(5), 317 (1985), (in Japanese).
11. H. Wiegand and H. Vetter, *Kunststoffe*, **56**(11), 761 (1966).
12. M. Takeshima and N. Funakoshi, *Proc. SID*, **25**(3), 219 (1984).

Received February 12, 1985
Accepted July 1, 1985